

Configurational lattice dynamics and hybrid Monte Carlo approaches to thermodynamic properties of solid solutions[☆]

N.L. Allan^{a,*}, G.D. Barrera^b, R.M. Fracchia^c, B.K. Pongsai^a, J.A. Purton^d

^a*School of Chemistry, University of Bristol, Cantock's Close, Bristol BS8 ITS, UK*

^b*Departamento de Química, Universidad Nacional de la Patagonia SJB, Ciudad Universitaria, (9000) Comodoro Rivadavia, Argentina*

^c*Universidad de Buenos Aires, Facultad de Ciencias Exactas y Naturales, Departamento de Química Inorgánica, Analítica y Química Física, Pabellón 2, Ciudad Universitaria, (1428) Buenos Aires, Argentina*

^d*CLRC, Daresbury Laboratory, Warrington, Cheshire WA4 4AD, UK*

Abstract

We discuss two novel methods, configurational lattice dynamics and hybrid Monte Carlo, recently proposed by us for the calculation of the thermodynamic properties of solid solutions. Results are presented for the mixing of MnO/MgO, CaO/MgO, RbCl/KCl, ZrO₂/CaO and MgSiO₃/MnSiO₃. It is crucial to sample many different configurations and allow explicitly for the relaxation of the local environment of each ion. Our methods are readily generalised to high temperatures and high pressures, and the study of phase transitions. © 2000 Elsevier Science B.V. All rights reserved.

Keywords: Lattice dynamics; Monte Carlo; Solid solutions; Enthalpy of mixing; Oxides

1. Introduction

Solid solutions and grossly non-stoichiometric compounds present particular challenges to the theoretician. Although substantial progress has been achieved in understanding structural and thermodynamic aspects of periodic, ordered materials and minerals (for example, see Ref. [1]), work on disordered ionic solids has most often been restricted to the dilute limit and involved point defect calculations, using, for example, the Mott-Littleton two-region approach (see the special issue, Ref. [2]). Such calculations are not readily extended to solid solutions or disordered systems containing a *finite* impurity or

defect content, restricting such an approach to end-member compounds. Studies of many industrially important ceramics and naturally occurring minerals are thereby excluded. In particular, an understanding of the thermodynamics of solid solutions of oxides, which are often strongly non-ideal, is essential for much of solid-state chemistry and mineralogy, including inorganic geochemistry, ceramic fabrication and design, solid-state batteries and heterogeneous catalysis. In addition, thermodynamic behaviour at elevated temperatures and also under high pressure is especially important for sustained material performance and for the stability of minerals deep within the mantle of the Earth.

In this paper we present results using two new techniques we have recently developed to tackle such problems. The first involves the direct minimisation of the free energy via lattice dynamics of a large number of possible configurations, which we refer to as configurational lattice dynamics, and the second a

[☆] Presented at the 5th World Congress of Theoretically Oriented Chemists (WATOC), Imperial College, London, 1–6 August, 1999.

* Corresponding author. Tel.: +44-117-928-8308; fax: +44-117-925-1295.

E-mail address: n.l.allan@bristol.ac.uk (N.L. Allan).

hybrid Monte Carlo (HMC) technique allowing an efficient sampling of a large number of different configurations. In ionic and semi-ionic solids it is crucial to allow for the strong coupling between the distribution of the ions and the relaxation of the local atomic environment around impurity ions and clusters of impurity ions. Relaxation energies for defect pairs and larger clusters may be of the order of several eV, are not additive and these contributions cannot be predicted simply from the separate relaxation around the isolated impurities. Thermal effects are allowed for explicitly in both techniques, which are also readily extended to high pressures.

Examples considered include solid solutions where the two cations involved are isovalent and fairly similar in size (e.g. MnO/MgO, RbCl/KCl, MgSiO₃/MnSiO₃), where there is a marked difference in size, but not in charge (CaO/MgO), and finally where there is a substantial mismatch in both size and charge (ZrO₂/CaO). Properties examined include entropies of mixing (CaO/MgO) and phase transitions at high pressure (MgSiO₃/MnSiO₃).

Taken together this set of examples form an excellent test of our approach since any proposed method must be sufficiently robust for the extensive relaxations accompanying the interchange of ions that are not only very different in size but which also do not possess the same charge.

2. Theoretical methods

2.1. Lattice dynamics

We use a recently developed, efficient method [3] which uses lattice statics and quasiharmonic lattice dynamics (QLD) for the fully dynamic structure optimisation of large unit cells via the analytic calculation of the free energy and its derivatives with respect to all strains [4]. Numerical differentiation of the free energy with respect to all the internal coordinates is normally prohibitively expensive. We calculate the full set of free energy first derivatives analytically and so, for the first time, a full minimisation of the quasiharmonic free energy with respect to all structural variables for large unit cells is possible.

In the quasi-harmonic approximation it is assumed

that the Helmholtz free energy of a crystal F , at a temperature T can be written as the sum of static and vibrational contributions,

$$F(\mathcal{E}, T) = \Phi_{\text{stat}}(\mathcal{E}) + F_{\text{vib}}(\mathcal{E}, T) \quad (1)$$

Φ_{stat} is the potential energy of the static lattice in a given state of strain \mathcal{E} , and F_{vib} is the sum of harmonic vibrational contributions from all the normal modes. For a periodic structure, the frequencies $\nu_j(\mathbf{q})$ of modes with wavevector \mathbf{q} are obtained by diagonalisation of the dynamical matrix $D(\mathbf{q})$ (For example, Ref. [5]). F_{vib} is given by

$$F_{\text{vib}} = \sum_{\mathbf{q}, j} \left\{ \frac{1}{2} h \nu_j(\mathbf{q}) + k_{\text{B}} T \ln[1 - \exp(-h \nu_j(\mathbf{q})/k_{\text{B}} T)] \right\} \quad (2)$$

in which the first term is the zero-point energy. The associated vibrational entropy S , is

$$S = \sum_{\mathbf{q}, j} \left\{ \frac{(h \nu_j(\mathbf{q})/T)}{\exp(h \nu_j(\mathbf{q})/k_{\text{B}} T) - 1} - k_{\text{B}} \ln[1 - \exp(-h \nu_j(\mathbf{q})/k_{\text{B}} T)] \right\}. \quad (3)$$

For a macroscopic crystal the sum over \mathbf{q} becomes an integral over a cell in reciprocal space, which can be evaluated by taking successively finer uniform grids (For example, Ref. [6]) until convergence is achieved. The free energy thus obtained is a function of both macroscopic (η_{λ}) and internal strains (ϵ_k), and it is simplest to treat the ϵ_k as thermodynamic variables on the same footing as the η_{λ} , comprising a total set of strain variables [7] denoted by \mathcal{E}_{Λ} . The equilibrium structure at an applied pressure P_{ext} , is then that which minimises the availability [8] $\tilde{G} = F + P_{\text{ext}} V$ with respect to all strains.

The minimisation of $F + P_{\text{ext}} V$ and subsequent thermodynamic manipulation can of course in principle be carried out by brute force, from numerical values of F obtained using Eq. (2). However, for large unit cells with many internal coordinates that are not determined by symmetry constraints it is much more efficient to use analytic expressions for the derivatives of F with respect to strain. The strain

derivatives are given by

$$\left(\frac{\partial F_{\text{vib}}}{\partial \mathcal{E}_A}\right)_{\mathcal{E}', T} = \sum_{\mathbf{q}, j} \left\{ \frac{h}{2\nu_j(\mathbf{q})} \left(\frac{1}{2} + \frac{1}{\exp(h\nu_j(\mathbf{q})/k_B T) - 1} \right) \left(\frac{\partial \nu_j^2(\mathbf{q})}{\partial \mathcal{E}_A} \right)_{\mathcal{E}'} \right\} \quad (4)$$

where the subscript \mathcal{E}' denote that all the \mathcal{E} are kept constant except for the differentiation variable. Derivatives of the frequencies are thus required. In our new code SHELL [3] the derivatives $(\partial \nu_j^2(\mathbf{q})/\partial \mathcal{E}_A)_{\mathcal{E}'}$ are obtained from the analytic expressions for the derivatives $(\partial D/\partial \mathcal{E}_A)_{\mathcal{E}'}$ by first-order perturbation theory. Full expressions for two- and three-body short-range potentials and for the Ewald summation are given in Refs. [4,9]. For obtaining derivatives the perturbation is infinitesimal and so the procedure is exact. No special consideration needs to be given to degeneracies in first order perturbation theory for thermodynamic properties, because the trace of $(\partial D/\partial \mathcal{E}_A)_{\mathcal{E}'}$ is invariant for any complete normal set of eigenvectors of D .

To obtain the equilibrium structure and Gibbs energy our new code uses a modified variable metric method [10] for minimising $F + P_{\text{ext}}V$ with respect to the \mathcal{E}_A . In the initial configuration the static energy Hessian, $(\partial^2 \Phi_{\text{stat}}/\partial \mathcal{E}_A \partial \mathcal{E}_B)$, which is a good approximation to $(\partial^2 F/\partial \mathcal{E}_A \partial \mathcal{E}_B)$, is calculated from its analytic expression, and its inverse together with the $(\partial F/\partial \mathcal{E}_A)$ is used to obtain an improved approximation to the minimum. In subsequent iterations the $(\partial F/\partial \mathcal{E}_A)$ are calculated and the inverse Hessian is updated by the BFGS formula [11]. An optimisation therefore requires one static Hessian calculation, and a small number of dynamic gradient calculations.

The quasi-harmonic approximation breaks down with increasing amplitude of vibration and hence at high temperatures. In general the quasi-harmonic approximation is usually valid up to temperatures of approximately one-half to two-thirds of the melting point. For any given temperature, higher pressures correspond to smaller internuclear separations and thus amplitudes of vibration and so the breakdown of the quasiharmonic approximation is often less important for applications involving high pressure.

The accurate calculation of the free energy via

QLD is fast and computationally efficient [3] and does not resort to lengthy thermodynamic integration. It is also an attractive strategy for temperatures below the Debye temperature where classical Monte Carlo fails due to the neglect of quantum effects. Our configurational lattice dynamics approach to solid solutions thus involves thermodynamic averaging over the results of a (limited) set of free-energy minimisations of different arrangements of the cations within a supercell. Previous work has often assumed just *one* (the most regular) arrangement and calculated its energy, with or possibly without relaxation, either by using lattice statics or by an ab initio method (For example, Ref. [12]).

Given the free energy G_k , for the relaxed structure of each possible cation arrangement k we then average using

$$\langle H \rangle = \frac{\sum_k H_k \exp(-\beta G_k)}{\sum_k \exp(-\beta G_k)} \quad (5)$$

$$\langle S \rangle = \frac{\sum_k H_k \exp(-\beta G_k)}{T \sum_k \exp(-\beta G_k)} + k_B \ln \sum_k \exp(-\beta G_k). \quad (6)$$

2.2. Hybrid Monte Carlo

The hybrid Monte Carlo approach [13,14] we have developed is related to that used in the modelling of polymers and biomolecules (see for example, Ref. [15]). During one HMC cycle, one of three options is chosen at random, with equal probability. The first of these is a short NVE molecular dynamics (MD) simulation (15 steps, timestep 1.5 fs) in which the last configuration is accepted or rejected by comparing its energy with the energy of the starting configuration and using the standard Metropolis algorithm [16]. If the last configuration is rejected, the original configuration is included in the statistical averaging of thermodynamic properties. In the second, a short MD run follows a random exchange of atoms. Again, the difference in energy between the previous configuration and that immediately after the MD simulation is used in the Metropolis algorithm. At the start of each MD run, velocities are chosen anew at random from a

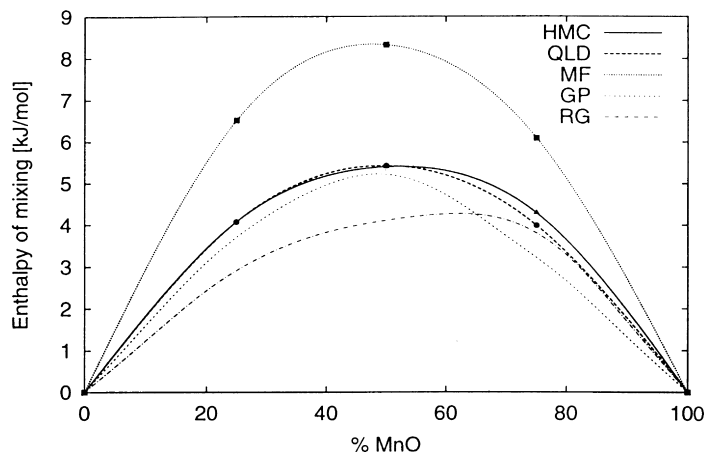


Fig. 1. Calculated values of ΔH_{mix} at 1300 K for MnO/MgO using hybrid Monte Carlo (HMC) (triangles), mean field theory (MF) (squares), and configurational quasiharmonic lattice dynamics (QLD) (circles). Two sets of experimental data (GP from Ref. [21] (.....), RG from Ref. [20] (---)) are also shown.

Maxwellian distribution. The third option is a random change of the volume of the box [17] which again is accepted or rejected using the Metropolis algorithm. We have discussed previously [14] the importance of the MD run in the second option; without this, ion exchanges are almost completely rejected and different configurations are not sampled.

Our lattice dynamics and HMC programs currently use conventional two- and three-body, rigid-ion and shell-model [18] potentials.

3. Results and discussion

3.1. MnO/MgO

We show values of ΔH_{mix} for MnO/MgO in Fig. 1. These were determined using (a) QLD and a unit cell of 64 atoms and 32 randomly-chosen cation arrangements, and (b) HMC and a box-size of 216 ions at 1300 K. All potentials are from Ref. [19]. The cell size and the number of cation arrangements in the

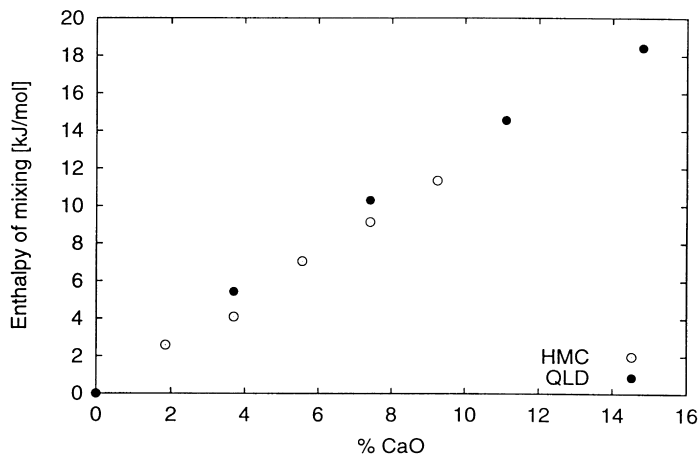


Fig. 2. Calculated values of ΔH_{mix} at 1800 K for CaO/MgO calculated using HMC and QLD simulations.

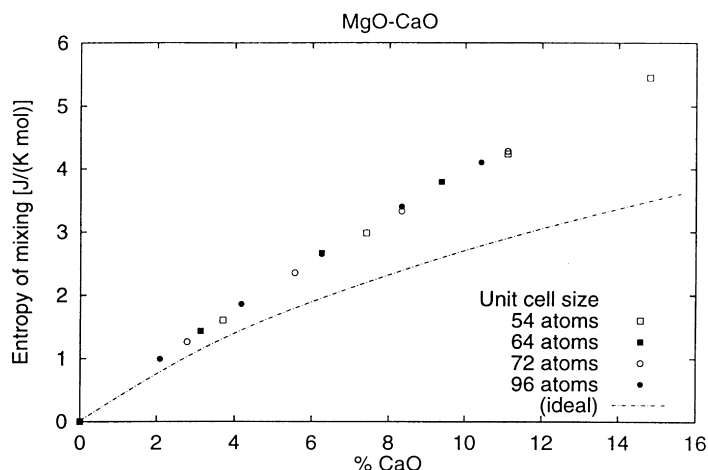


Fig. 3. Calculated values of ΔS_{mix} at 1800 K for CaO/MgO calculated using QLD. For comparison the ideal entropy of mixing is also shown (dotted line).

configurational lattice dynamics calculations is sufficient to ensure convergence in ΔH_{mix} to 0.1 kJ mol^{-1} . The enthalpies of mixing for 32-ion cells (averaging again over 32 configurations) and 64-ion cells are almost identical and substantially smaller than those from a 16-ion cell (all possible cation arrangements). It is particularly satisfying that there is excellent agreement between the QLD and HMC methods.

The calculated enthalpy of mixing at 1300 K is symmetric with a maximum of approximately 5.4 kJ mol^{-1} (50% MgO, 50% MnO). Agreement with the data of Gripenberg et al. [20] is good, but the results show none of the asymmetry reported by Raghavan [21]; no constraints as to this symmetry have of course been imposed in the calculations.

For comparison values calculated using a mean field approach are also plotted in Fig. 1. Instead of separate, distinct Mn^{2+} and Mg^{2+} ions, a “hybrid” ion is introduced, for which the non-Coulombic potentials are a linear combination of the potentials for Mn^{2+} and Mg^{2+} , weighted by the site occupancies appropriate to the particular overall composition considered. When local relaxation or clustering is important, these mean-field results are expected to be poor. Fig. 1 shows that this occurs even here, where the Mn^{2+} and Mg^{2+} ions are not too dissimilar in size (0.83 and 0.72 Å, respectively).

3.2. CaO/MgO

We now turn to $\text{Ca}_x\text{Mg}_{1-x}\text{O}$ ($0 < x < 0.15$), where the size mismatch between the two different cations is much greater (1.00 and 0.72 Å) than in the previous example. Fig. 2 shows enthalpies of mixing calculated using both QLD and HMC at 1800 K, and the set of potentials from Ref. [19]. The QLD results are for a cell of 54 atoms and 50 randomly chosen configurations. With this number of atoms we obtain convergence to 0.1 kJ mol^{-1} with respect to increasing cell size; for this size of cell, 70 configurations gives typically the same convergence with respect to the number of configurations. There is good agreement between the QLD and HMC values, with the differences possibly due to anharmonic terms not taken into account in the QLD calculation.

The agreement between the HMC enthalpy of mixing and that obtained from the QLD, using only 50 configurations is such that we have extended the QLD approach and evaluated entropies of mixing for this system using Eq. (6). Entropies of mixing, calculated using QLD, for $\text{Ca}_x\text{Mg}_{1-x}\text{O}$ at 1800 K, using cell sizes of 54, 64, 72 or 96 atoms and 95 randomly chosen configurations, are shown in Fig. 3. The corresponding figure for 120 configurations is indistinguishable by eye. The QLD approach produces adequate convergence even for ΔS_{mix} with relatively small cells. ΔS_{mix} includes *both* configurational *and*

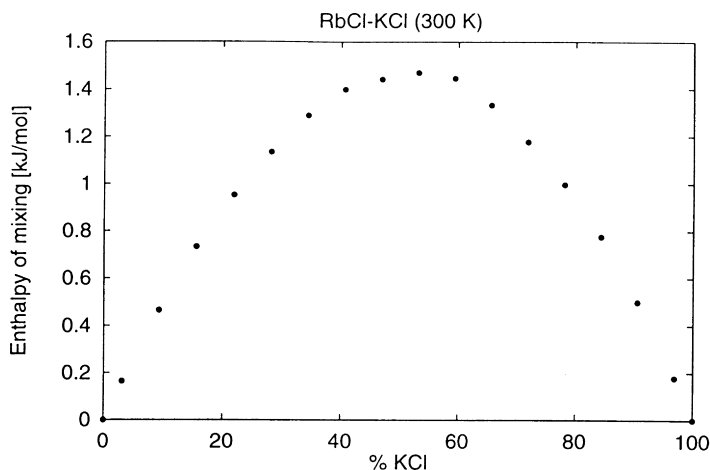


Fig. 4. Calculated values of ΔH_{mix} at 300 K for RbCl/KCl calculated using QLD.

vibrational contributions. Here the vibrational contribution is positive since it is dominated by the heavier mass of the Ca ion and the expansion of the lattice it produces, both of which tend to decrease frequencies and overall ΔS_{mix} is larger than the “ideal” value. Overall the total entropy of mixing for $\text{Ca}_x\text{Mg}_{1-x}\text{O}$ is larger than the “ideal” entropy of mixing, also plotted in Fig. 3.

3.3. RbCl/KCl

For comparison we have also studied the mixed halide system RbCl/KCl. The difference in size between the two different cations is somewhat larger

(ionic radii 1.48 and 1.33 Å) than between Mn^{2+} and Mg^{2+} . Figs. 4 and 5 show enthalpies and entropies of mixing calculated using QLD at 300 K, and interionic potentials from Ref. [22], for a cell size of 64 atoms and 20 configurations. The enthalpies of mixing are small and it is possible the calculated values could show a marked dependence on the potential model employed. The total entropy of mixing at 300 K, again the sum of vibrational and configurational contributions, is slightly smaller than the ideal value, in contrast to CaO/MgO at 1800 K. There appear to be no experimental data for comparison.

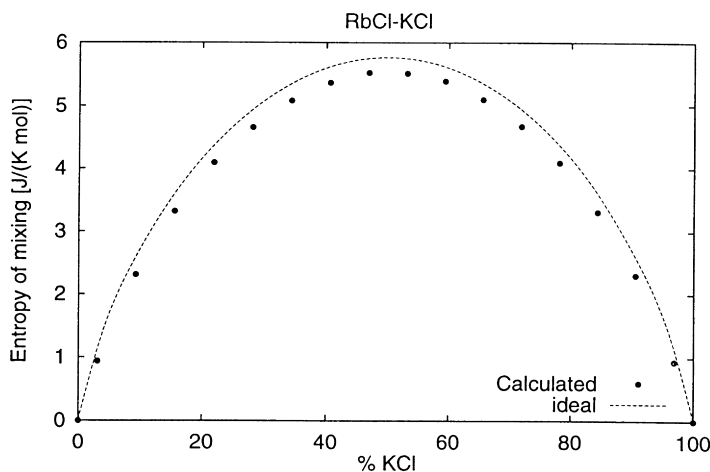


Fig. 5. Calculated values of ΔS_{mix} at 300 K for RbCl/KCl calculated using QLD. For comparison the ideal entropy of mixing is also shown (dotted line).

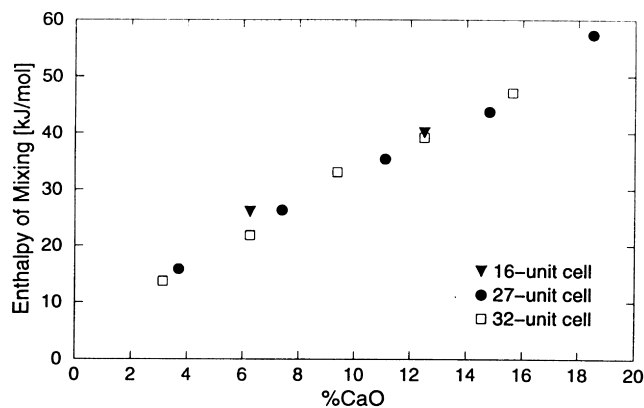


Fig. 6. Calculated values of ΔH_{mix} at 200 K for ZrO_2/CaO calculated using QLD.

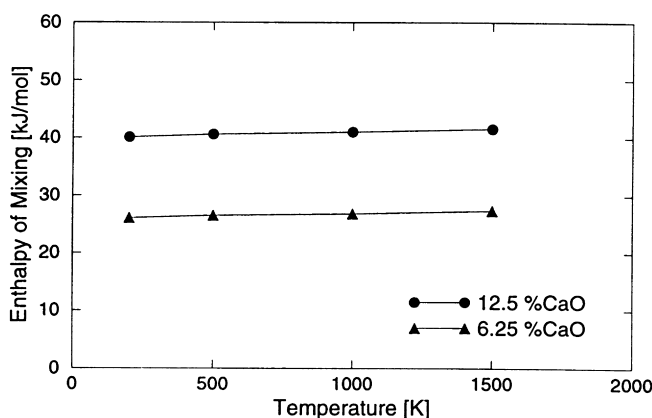
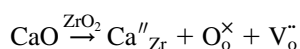


Fig. 7. ΔH_{mix} vs. T for ZrO_2/CaO , calculated using QLD and a 16-unit cell, over the temperature range 200–1500 K.

3.4. ZrO_2/CaO

The system ZrO_2/CaO , which exhibits high oxygen ion conductivity, presents a particular challenge for our methods since it is the first example we have studied involving heterovalent doping, and hence disorder on both cation and anion sublattices. It is also well established, from both theory (e.g. Refs. [23–25]) and EXAFS studies [26,27], that defect clustering is particularly important in doped zirconia. For every Ca^{2+} incorporated into ZrO_2 , an oxygen vacancy is also introduced as a charge-compensating defect according to



The configurational lattice dynamics calculations thus

have to include configurations generated from both randomly chosen cation and anion arrangements. At this stage we have confined ourselves to a study of the enthalpy of mixing of the (hypothetical) reaction involving the formation of $\text{Zr}_{1-x}\text{Ca}_x\text{O}_{2-x}$ from CaO and (hypothetical) *cubic*- ZrO_2 (fluorite structure). We use potentials taken from a consistent set of electron-gas potentials derived for heterovalent dopants in high-temperature superconducting oxides [28].¹

Fig. 6 shows that satisfactory convergence in ΔH_{mix} is obtained even for $\text{Zr}_{1-x}\text{Ca}_x\text{O}_{2-x}$ ($0 < x < 0.2$), where lattice relaxation is extensive, with relatively

¹ The potentials for ZrO_2 in Ref. [24] give rise to imaginary frequencies at 200 K, thus rendering them invalid for use at this and higher temperatures.

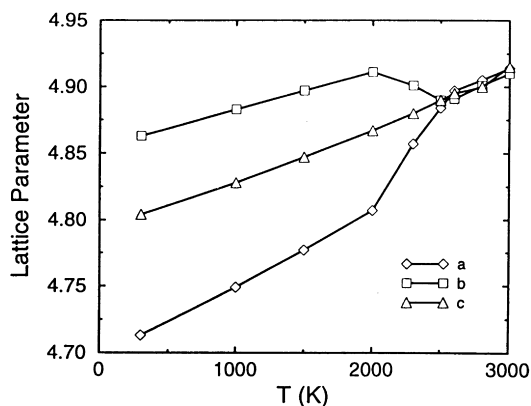


Fig. 8. Lattice parameters (Å) vs. T (K) at 20 GPa for $\text{Mg}_{0.6}\text{Mn}_{0.4}\text{SiO}_3$.

small cell sizes. In this figure we denote a cell originally comprising y ZrO_2 formula units before the introduction of Ca^{2+} ions (and an equal number of oxygen vacancies) as a y -unit cell. Results from QLD at 200 K using various cell sizes (300, 450 and 600 configurations for 16-, 27- and 32-unit cells respectively) are plotted. Fig. 7 shows the calculated temperature dependence of ΔH_{mix} over the temperature range 200–1500 K calculated using a 48-atom cell and 300 configurations. ΔH_{mix} does not vary significantly with temperature, which supports the common assumption that ΔH_{mix} is largely temperature independent. Preliminary results indicate that ΔS_{mix} is larger than the ideal value, as for CaO-MgO.

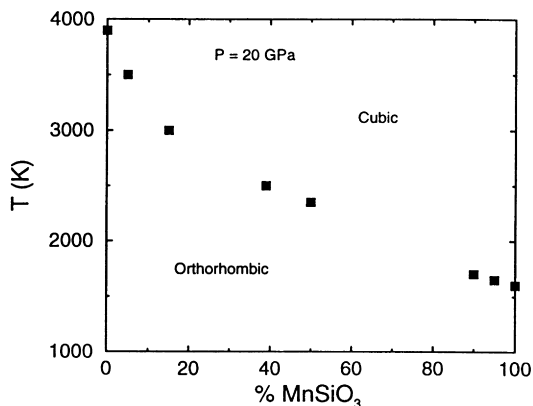


Fig. 9. Calculated orthorhombic–cubic transition temperature (K) at 20 GPa vs. Mn content.

3.5. $\text{MgSiO}_3/\text{MnSiO}_3$ —phase transitions

A valuable feature of the HMC technique is that it can be readily used to examine the influence of high impurity or defect concentrations on phase transitions. Alternative methods such as the use of an Ising-type Hamiltonian cannot only average out local effects such as ion association but are not readily extended to include the effects of lattice vibrations and high pressure. Since Mn–Mg mixing in silicates is expected to be quite non-ideal (see for example, Ref. [29]), as in the binary oxides we have already considered, we have chosen to examine (Mg, Mn) SiO_3 perovskite [30]. Parameterisation of approximate Hamiltonians becomes increasingly complex for such compounds beyond binary and pseudobinary mixtures.

We used the same set of interionic potentials for MgSiO_3 as for Mg_2SiO_4 in Ref. [31]². The HMC runs are for a simulation cell of 540 ions ($3 \times 3 \times 3$ unit cells), with an equilibration period of 50,000 cycles and averaging enthalpy and structural data over a further 50,000 cycles. Matsui and Price [31] have used constant-pressure MD to show that above 10 GPa, orthorhombic MgSiO_3 undergoes a temperature induced phase transition to a cubic phase prior to melting, whereas at lower pressures the orthorhombic phase melts without any change of solid phase. For MgSiO_3 itself, HMC results are very similar. The calculated transition temperature from the orthorhombic to the cubic phase is 3900 K at 20 GPa. Fig. 8 shows the variation of the lattice parameters of $\text{Mg}_{0.6}\text{Mn}_{0.4}\text{SiO}_3$ with temperature, which shows this compound also undergoes such a phase transition at this temperature. The transition temperature (2500 ± 50 K) is lower than for MgSiO_3 , in keeping with simple radius ratio arguments. The calculated transition temperature at 20 GPa as a function of Mn composition is displayed in Fig. 9. It is evident that a linear interpolation between the end members is a very poor approximation since the orthorhombic–cubic phase transition for $\text{Mg}_{0.6}\text{Mn}_{0.4}\text{SiO}_3$ is 500 K lower than the value of ≈ 3000 K predicted by such an interpolation. It is worth noting that, unlike the transition temperature, the calculated volume as a function of Mn composition shows only a small

² The experimental evidence is contradictory [32,33].

positive deviation from Vegard's Law, since the a lattice parameter has a positive deviation and the other two negative deviations. We have not been able to find experimental data for comparison; data are particularly sparse at high temperatures and high pressures. If the analogous compound $(\text{Mg,Fe})\text{SiO}_3$ were to exhibit such a phase transition [32,33] there would be important implications for the thermodynamic and compositional modelling of the Earth's mantle.

4. Conclusions

We have shown how the configurational lattice dynamics and HMC methods provide an attractive route to an accurate description of the thermodynamics of mixing of ionic solids. It is essential to take explicit account of the (optimised) local environment around each cation and anion in the solid solution, i.e. ionic relaxation without any averaging out of such local effects. Unlike existing techniques, such as the use of a parameterised Ising Hamiltonian, our methodologies are generally applicable to a wide range of materials and minerals, high pressures and elevated temperatures and lattice dynamics can also be used under conditions where classical simulations fail. Considerable work, both methodological and computational, remains in order to make these two techniques generally applicable and this is currently underway in our laboratories.

Acknowledgements

This work was funded by NERC grants GR9/02621, EPSRC grants GR/L31340 and GR/M34799. GDB gratefully acknowledges financial support from el Consejo Nacional de Investigaciones Científica y Técnicas de al Republica Argentina and a Fundación Antorchas grant. We would like to thank Mark Taylor and Hugh Barron for useful discussions.

References

- [1] Computer Modelling in Inorganic Crystallography, in: C.R.A. Catlow (Ed.), Academic Press, San Diego, London, 1996.
- [2] J. Chem. Soc., Faraday Trans 2, 85 (1989) 335.

- [3] M.B. Taylor, G.D. Barrera, N.L. Allan, T.H.K. Barron, W.C. Mackrodt, *Comp. Phys. Commun.* 109 (1998) 135.
- [4] M.B. Taylor, G.D. Barrera, N.L. Allan, T.H.K. Barron, *Phys. Rev. B* 56 (1997) 14380.
- [5] D.C. Wallace, *Thermodynamics of Crystals*, Wiley, New York, 1972.
- [6] D.J. Chadi, M.L. Cohen, *Phys. Rev. B* 8 (1973) 5747.
- [7] T.H.K. Barron, T.G. Gibbons, R.W. Munn, *J. Phys. C* 4 (1971) 2805.
- [8] A.B. Pippard, *The Elements of Classical Thermodynamics*, Cambridge University Press, Cambridge, 1964.
- [9] M.B. Taylor, N.L. Allan, J.A.O. Bruno, G.D. Barrera, *Phys. Rev. B* 59 (1999) 353.
- [10] P.J. Harley, in: J.L. Mohamed, J.E. Walsh (Eds.), *Numerical Algorithms*, Clarendon Press, Oxford, 1986, p. 239.
- [11] W.H. Press, S.A. Teukolsky, W.T. Vetterling, B.P. Flannery, *Numerical Recipes in Fortran*, 2nd ed., Cambridge University Press, Cambridge, 1992 (420pp).
- [12] K.D. Health, W.C. Mackrodt, V.R. Saunders, M. Causà, *J. Mater. Chem.* 4 (1994) 825.
- [13] J.A. Purton, J.D. Blundy, M.B. Taylor, G.D. Barrera, N.L. Allan, *Chem. Commun.* (1998) 627.
- [14] J.A. Purton, G.D. Barrera, N.L. Allan, J.D. Blundy, *J. Phys. Chem. B* 102 (1998) 5202.
- [15] M.E. Clamp, P.G. Baker, C.J. Stirling, A. Brass, *J. Comp. Chem.* 15 (1994) 838.
- [16] N.I. Metropolis, A.W. Rosenbluth, M.N. Rosenbluth, A.H. Teller, E. Teller, *J. Chem. Phys.* 21 (1953) 1087.
- [17] Q. Wang, J.K. Johnson, J.Q. Broughton, *Mol. Phys.* 89 (1996) 1105.
- [18] B.G. Dick, A.W. Overhauser, *Phys. Rev.* 112 (1958) 90.
- [19] G.V. Lewis, C.R.A. Catlow, *J. Phys. C. Solid State Phys.* 18 (1985) 1149.
- [20] S. Raghavan, PhD Thesis, Indian Institute of Science, Bangalore, India, 1971.
- [21] H. Gripenberg, S. Seetharaman, L.I. Staffansson, *Chem. Scr.* 13 (1978/79) 162.
- [22] W.C. Mackrodt, R.F. Stewart, *J. Phys. C* 12 (1979) 431.
- [23] W.C. Mackrodt, P.M. Woodrow, *J. Am. Ceram. Soc.* 69 (1986) 277.
- [24] A. Dwivedi, A.N. Cormack, *Philos. Mag.* A 61 (1990) 1.
- [25] M.S. Khan, M.S. Islam, D.R. Bates, *J. Mater. Chem.* 8 (1998) 2299.
- [26] C.R.A. Catlow, A.V. Chadwick, G.N. Greaves, L.M. Moroney, *J. Am. Ceram. Soc.* 69 (1986) 272.
- [27] M. Cole, C.R.A. Catlow, J.P. Dragun, *J. Phys. Chem. Solids* 51 (1990) 507.
- [28] N.L. Allan, W.C. Mackrodt, *Adv. Solid State Chem.* 3 (1993) 221.
- [29] B.J. Wood, R.T. Hackler, D.P. Dobson, *Contrib. Miner. Petrol.* 115 (1994) 735.
- [30] J.A. Purton, N.L. Allan, J.D. Blundy, *Chem. Commun.* (1999) 707.
- [31] M. Matsui, G.D. Price, *Nature* 351 (1991) 735.
- [32] E. Knittle, R. Jeanloz, *Science* 235 (1987) 668.
- [33] C. Meade, H.K. Mao, J. Hu, *Science* 268 (1995) 1743.